

Unravelling the Reaction Path of Rhodium–MonoPhos-Catalysed Olefin Hydrogenation**

Elisabetta Alberico,^{*,[a]} Wolfgang Baumann,^{*,[b]} Johannes G. de Vries,^{*,[c]}
Hans-Joachim Drexler,^[b] Serafino Gladiali,^[d] Detlef Heller,^[b]
Huub J. W. Henderickx,^[c] and Laurent Lefort^[c]

Dedicated to Professor Christian Bruneau on the occasion of his 60th birthday

Abstract: The mechanism of the asymmetric hydrogenation of methyl (Z)-2-acetamidocinnamate (mac) catalysed by $[\text{Rh}(\text{MonoPhos})_2(\text{nbd})]\text{SbF}_6$ (MonoPhos: 3,5-dioxa-4-phosphacyclohepta[2,1-a:3,4-a']dinaphthalen-4-yl)dimethylamine) was elucidated by using ^1H , ^{31}P and ^{103}Rh NMR spectroscopy and ESI-MS. The use of nbd allows one to obtain in pure form the rhodium complex that contains two units of the ligand. In contrast to the analogous complexes that contain *cis,cis*-1,5-cyclooctadiene (cod), this complex shows well-resolved NMR spectroscopic signals. Hydrogenation of these catalyst precursors at 1 bar total pressure gave rise to the formation of a bimetallic complex of general formula $[\text{Rh}$ -

(MonoPhos) $_2](\text{SbF}_6)_2$; no solvate complexes were detected. In the dimeric complex both rhodium atoms are ligated to two MonoPhos ligands but, in addition, each rhodium atom also binds to one of the binaphthyl rings of a ligand that is bound to the other rhodium metal. Upon addition of mac, a mixture of diastereomeric complexes $[\text{Rh}(\text{MonoPhos})_2(\text{mac})]\text{SbF}_6$ is formed in which the substrate is bound in a chelate fashion to the metal. Upon hydrogenation, these adducts are converted into a new complex $[\text{Rh}$ -

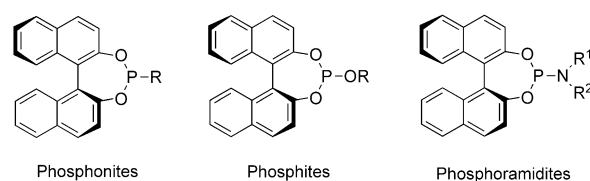
(MonoPhos) $_2[\text{mac}(\text{H})_2]\text{SbF}_6$ in which the methyl phenylalaninate $\text{mac}(\text{H})_2$ is bound through its aromatic ring to rhodium. Addition of mac to this complex leads to displacement of the product by the substrate. No hydride intermediates could be detected and no evidence was found for the involvement at any stage of the process of complexes with only one coordinated MonoPhos. The collected data suggest that the asymmetric hydrogenation follows a Halpern-like mechanism in which the less abundant substrate–catalyst adduct is preferentially hydrogenated to phenylalanine methyl ester.

Keywords: asymmetric catalysis • dimers • phosphoramidites • reactive intermediates • rhodium

Introduction

Asymmetric hydrogenation is one of the most attractive areas of enantioselective homogeneous catalysis.^[1] Recently, it has received new impetus through the discovery that monodentate ligands^[2] such as BINOL-based (BINOL = 1,1'-bi-2-naphthol) C_1 -symmetric phosphonites,^[2c] phosphites^[2d] and phosphoramidites^[2e] can provide very efficient catalysts, thus turning around the long-established belief that only chelating bidentate ligands are properly suited for ensuring high stereoselectivities (Scheme 1).

The easier and straightforward synthesis of these monodentate ligands, compared to their bidentate counterparts,



Scheme 1. Binaphthol-based monodentate P-donor ligands.

[a] Dr. E. Alberico

Istituto di Chimica Biomolecolare
Consiglio Nazionale delle Ricerche
trav. La Crucca 3, 07040 Sassari (Italy)
Fax: (+39) 079 284 1299
E-mail: Elisabetta.Alberico@cnr.it

[b] Priv.-Doz. Dr. W. Baumann, Dr. H.-J. Drexler, Prof. Dr. D. Heller

Leibniz-Institut für Katalyse e.V. an der Universität Rostock
Albert-Einstein-Strasse 29A, 18059 Rostock (Germany)
E-mail: Wolfgang.Baumann@catalysis.de

[c] Prof. Dr. J. G. de Vries, H. J. W. Henderickx, Dr. L. Lefort

DSM Resolve and DSM Innovative Synthesis BV
a unit of DSM Pharma Chemicals, P.O. Box 18
6160 MD Geleen (The Netherlands)
E-mail: Hans-JG.Vries-de@dsm.com

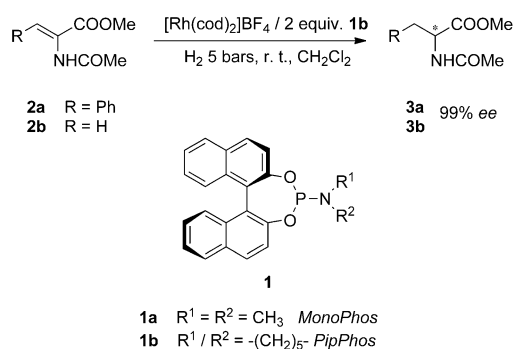
[d] Prof. Dr. S. Gladiali

Dipartimento di Chimica, Università di Sassari
via Vienna 2, 07100 Sassari (Italy)

[**] MonoPhos: 3,5-Dioxa-4-phosphacyclohepta[2,1-a:3,4-a']dinaphthalen-4-yl)dimethylamine.

Supporting information for this article is available on the WWW under <http://dx.doi.org/10.1002/chem.201101793>.

has opened new possibilities such as the parallel synthesis of large ligand libraries^[3] and the combinatorial screening of heterocombinations of monodentate ligands in the search for the best catalyst for a given substrate.^[3b,4] Compared to the state of the art reached with bidentate ligands,^[5] readily accessible and stable monodentate phosphoramidites can lead to both higher rates and/or higher enantioselectivities in the rhodium-catalysed asymmetric hydrogenation of α - and β -dehydroamino acid derivatives, for which *ee* values higher than 99% have been achieved (Scheme 2).^[6]



Scheme 2. Rh/phosphoramidite-catalysed asymmetric hydrogenation of α -dehydroamino acid esters.

The use of Rh-monodentate phosphoramidite catalysts has been recently commercialised by DSM: the bulky phosphoramidite ligand **6** (Scheme 3) in combination with a triarylphosphine **7** has been used in the Rh-promoted hydrogenation of the α -isopropylcinnamic acid derivative **4**. The product **5** is an intermediate en route to Aliskiren, an antihypertensive agent commercialised by Novartis, which represents the first example of an orally active renin inhibitor.^[7]

In view of the academic and industrial interest in these phosphoramidite-based catalysts, we set out to investigate the mechanism of the asymmetric hydrogenation of methyl (*Z*)-2-acetamidocinnamate **2a** (Scheme 2) promoted by rhodium complexes of **1a** (MonoPhos). Despite several earlier

studies,^[8–10] most mechanistic issues are still waiting for a convincing definition.^[11] A major one is the nature of the species that are obtained upon hydrogenation of [Rh-(MonoPhos)₂(diene)]BF₄ (diene = *cis,cis*-1,5-cyclooctadiene (cod) or bicyclo[2.2.1]hepta-2,5-diene (nbd)). The asymmetric hydrogenation of α -dehydroamino acid derivatives using rhodium with monodentate phosphoramidite, phosphite or phosphinites ligands only proceeds with high enantioselectivity if non-protic solvents are used such as CH₂Cl₂, ClCH₂CH₂Cl, EtOAc or THF, in contrast with rhodium/bis-phosphine catalysts that perform better in protic solvents such as methanol. In the latter case, hydrogenation of the catalyst precursor leads to a [Rh(bis-phosphine)(MeOH)₂]⁺X[–] species, which in some cases can be isolated.^[12] It remains in question if the use of chlorinated solvents such as CH₂Cl₂ can lead to the formation of such bis-solvato species. Another issue is the uncertainty with regards to the number of ligands that are ligated to rhodium during the crucial hydrogenation step in the catalytic cycle. There are conflicting reports in the literature about this (*vide infra*). In this paper, we report the results of a mechanistic study of the rhodium/MonoPhos dehydroamino acid hydrogenation, which aid in shedding some light on these challenging questions.

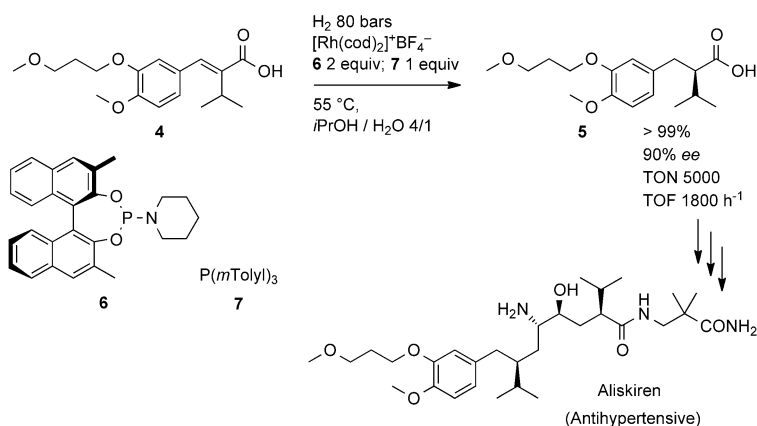
Results and Discussion

The mechanism of asymmetric hydrogenation catalysed by rhodium complexes with monodentate phosphorus ligands is poorly understood, and structural information on the intermediates formed in the catalytic cycle is scarce. Reetz and co-workers,^[8] by using density functional theory (DFT) calculations, found that hydrogenation of itaconic acid dimethyl ester with rhodium monodentate phosphite catalysts proceeds according to the lock-and-key mechanism, that is, the prevailing enantiomer of the product originates from the more abundant catalyst–substrate adduct formed in solution.^[13]

Even if a generalisation cannot be made because the situation can be different case by case, this is in contrast with

the most credited hydrogenation mechanism that involves rhodium-chelating diarylphosphine catalysts in which it is the less-abundant catalyst–substrate adduct that, due to its higher reactivity, leads to the prevailing enantiomer of the product.^[14]

The higher lability of monophosphines relative to chelating bidentate diphosphines may influence the dissociation equilibria in favour of unsaturated species, therefore one important aspect to be addressed concerns the number of monoden-



Scheme 3. Use of a Rh-monophosphoramidite catalyst for the synthesis of an intermediate for Aliskiren.

tate ligands coordinated to rhodium during catalysis. In the Rh-catalysed olefin hydrogenation using a monodentate phosphoramidite derived from a chiral spirodiol, Zhou et al. postulated the intermediacy of a rhodium substrate complex that contained only one molecule of the ligand.^[9]

However, this conclusion is in contrast with the observation of non-linear effects on the stereoselectivity as observed by the same authors with their ligand^[9] and by other authors with a different binaphthol-based monodentate phosphoramidite.^[11] Taken together with kinetic and NMR spectroscopy data, these facts better fit the hypothesis that two monodentate phosphoramidites are bound to rhodium in the active catalytic species.^[11] This proposal seems to be confirmed by recent findings by Gridnev, Fan and Pringle who, in the hydrogenation with monophosphonite–Rh catalysts, identified an intermediate such as $[\text{RhH}(\text{alkyl})\text{L}_2]^+$, which featured two ligands coordinated to rhodium during the catalytic cycle.^[10]

In the case of the rhodium/MonoPhos (**1a**) system, preliminary investigations by some of us have shown that when the ligand/Rh ratio is reduced from 2 to 1, the asymmetric hydrogenation of methyl (*Z*)-2-acetamidocinnamate (**mac**; **2a**) is faster while the enantioselectivity stays the same.^[11] Although this suggests that a complex that contains one single unit of ligand might be the active catalytic species, the authors explained the phenomenon in terms of an equilibrium between different $[\text{RhL}_n]^+$, with *n* varying from 0 to 4. Since the formation of inactive $[\text{RhL}_3]^+$ and $[\text{RhL}_4]^+$ is disfavoured at lower ligand/metal ratios, this could explain the higher rates observed. The single-ligand hypothesis was definitely disproven by subsequent work in which Rh complexes built up in situ from two different monodentate phosphoramidite ligands showed better performances than the counterparts built up from only one of the two phosphoramidites.^[4b] The investigations on this catalytic system are hampered by the fact that when $[\text{Rh}(\text{cod})_2]\text{BF}_4$ and 2.1 equiv of MonoPhos are mixed in dichloromethane at room temperature, several species are formed with a ligand to rhodium ratio that ranges from 1 to 4, this last one being formed in substantial amounts. However, it is possible to suppress the formation of the species $[\text{RhL}_3]^+$ and $[\text{RhL}_4]^+$ by slow addition of a solution of the ligand to the solution of the metal precursor. This allowed the isolation of $[\text{Rh}(\textbf{1a})_2(\text{cod})]\text{BF}_4$, which was contaminated with small amounts of $[\text{Rh}(\textbf{1a})(\text{cod})]\text{BF}_4$.^[15] Upon ^{31}P NMR spectroscopic analysis, two species with two coordinated MonoPhos ligands were identified that slowly interconverted at room temperature and showed broad absorptions. By lowering the temperature, it was possible to freeze out this equilibrium and to observe resolved peaks for each species. The two complexes are structural isomers that differ in the relative orientation of the two coordinated MonoPhos ligands. One of these complexes is *C*₂ symmetric with the dimethylamino groups of the phosphoramidites pointing in opposite direction, one above and the other below the plane defined by the metal and the two magnetically equivalent P donors. The second complex is *C*₁ symmetric with both the dimethylamino

groups pointing in the same direction of the coordination plane and with two non-equivalent P donors. A recent publication of Pringle and co-workers pointed out that the observation of two isomers is due to the restricted rotation of the two monodentate phosphorus ligands caused by the relatively bulky cyclooctadiene ligand.^[16] Norbornadiene is less bulky and thus in the analogous $[\text{RhP}_2(\text{nbd})]\text{BF}_4$, rotation is less hindered and hence resolved signals can be observed at room temperature. The ^{31}P and ^{103}Rh NMR spectroscopic data of these complexes are reported in Table 1 for the sake of comparison with the species that will be discussed later in this study.

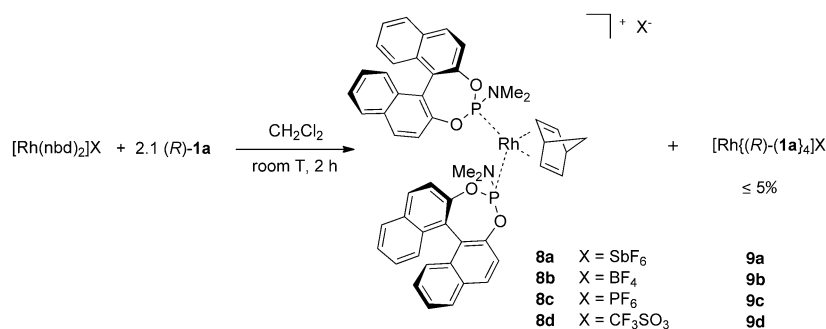
Table 1. ^{31}P and ^{103}Rh NMR data of $[\text{Rh}(\textbf{1a})(\textbf{R})\text{-MonoPhos}]_x(\text{cod})\text{BF}_4$ complexes (*x* = 1, 2).^{[a][15]}

Compound	Multiplet	$\delta(^{31}\text{P})$ [ppm]	$^1J(\text{P,Rh})$ [Hz]	$J(\text{P,P})$ [Hz]	$\delta(^{103}\text{Rh})$ [ppm]
$[\text{Rh}(\textbf{1a})(\text{cod})]\text{BF}_4$	d	141.4	239.0	–	–390.9
$[\text{Rh}(\textbf{1a})_2(\text{cod})]\text{BF}_4$	dd	139.5	242.0	39.6	–374.2
(<i>C</i> ₁ symmetrical)	dd	133.5	239.1	39.2	
$[\text{Rh}(\textbf{1a})_2(\text{cod})]\text{BF}_4$	d	137.4	231.8	–	[b]
(<i>C</i> ₂ symmetrical)					

[a] Spectra were recorded in CDCl_3 at 228 K. [b] This species could not be observed in the ^{103}Rh NMR spectrum: the corresponding signal in the ^{31}P NMR spectrum is broad, which might make the transfer of magnetisation and the detection of the signal in the ^{103}Rh NMR spectrum more difficult.

Because of the inability to isolate pure $[\text{Rh}(\textbf{1a})_2(\text{cod})]\text{BF}_4$ and in view of its broad ^{31}P NMR spectroscopic absorptions, the in situ prepared catalyst was not well-suited for mechanistic investigations.^[17] We were not able to render the synthesis of the Rh–MonoPhos complexes that contained cod more selective, but by replacing this diolefin with nbd we succeeded for the first time in isolating a well-defined catalyst precursor that contained two units of ligand.

Synthesis of catalyst precursors: When a solution of the ligand (*R*)-MonoPhos **1a** (2.1 equiv) in either THF or CH_2Cl_2 was added dropwise to a solution of the diolefin precursor $[\text{Rh}(\text{nbd})_2]\text{X}$ —with X being either BF_4^- , SbF_6^- , PF_6^- or CF_3SO_3^- —in the same solvent at room temperature, only one major species **8** was observed (Scheme 4).^[18] Complexes **8** share the same spectroscopic features, regardless of the counteranion. In the ^{31}P NMR spectrum, a single signal (only slightly broadened) is observed at about $\delta = 139$ ppm, which is a doublet as a result of the spin–spin coupling with the ^{103}Rh nuclide (free MonoPhos $\delta = 148.7$ ppm in CDCl_3). The coupling to rhodium is comparable for the various anions ($^1J(\text{Rh,P}) \approx 253.0$ Hz; Table 2). Consistent with the ^{31}P NMR spectrum, just one set of signals is observed in the ^1H NMR spectrum for the coordinated MonoPhos ligands (Figure 1). Within each ligand, however, the naphthyl groups are diastereotopic, and consequently 12 signals, one for each aromatic proton, are observable and also assignable (see Table SI3 in the Supporting Information). Four singlets, each accounting for two hydrogen atoms, are observed for the coordinated nbd, two for the olefinic $-\text{CH}=\text{}$, one for the



Scheme 4. Preparation of $[\text{Rh}\{(R)\text{-1a}\}_2(\text{nbd})]\text{X}$ catalyst precursors **8**.

Table 2. ^{31}P and ^{103}Rh NMR spectroscopy data of $[\text{Rh}\{(R)\text{-1a}\}_2(\text{nbd})]\text{X}$ complexes **8** in CDCl_3 .

Compound	Multiplet	$\delta(^{31}\text{P})$ [ppm]	$^1J(\text{P,Rh})$ [Hz]	$\delta(^{103}\text{Rh})$ [ppm]
8a	d	138.8	251.1	
8b	d	138.8	249.4	−268 ^[a]
8c	d	138.4	253.3	
8d	d	138.8	251.1	
1a	s	148.7		

[a] ^{103}Rh NMR spectrum was recorded on a sample dissolved in CD_2Cl_2 .

allylic $-\text{CH}-$ and one for the bridging $-\text{CH}_2-$. Whereas the coordinated double bonds are equivalent, within each double bond the two hydrogen atoms are not. In the $^1\text{H}, ^{103}\text{Rh}$ HMQC spectrum of complex $[\text{Rh}\{(R)\text{-1a}\}_2(\text{nbd})]\text{BF}_4$ (**8b**), the signal due to the rhodium(I) nucleus ($\delta(^{103}\text{Rh}) = -268$ ppm) is a triplet ($^1J(\text{Rh,P}) = 250$ Hz) indicative of the coupling to two equivalent phosphorus atoms (see Figure SI8 in the Supporting Information).

The stoichiometry of the $[\text{Rh}\{(R)\text{-1a}\}_2(\text{nbd})]\text{X}$ complexes **8** was confirmed by the integrated intensities of the signals in the ^1H NMR spectrum and further corroborated by ESI-MS. For each complex, the relative anion X^- was probed in

the negative-ion mode, whereas for the cation $[\text{Rh}\{(R)\text{-1a}\}_2(\text{nbd})]^+$, a common fragmentation pattern for all complexes in the positive-ion mode was observed which shows the molecular ion at m/z 913, a small peak due to loss of nbd at m/z 821 and the base peak that arises from the loss of a molecule of MonoPhos at m/z 554.

Despite several attempts, it was not possible to grow crystals of these complexes suitable for X-ray analysis. However, based on the NMR spectroscopy and ESI-MS results, it can be confidently stated that the synthesised complexes contain two ligands coordinated to rhodium and that they possess C_2 symmetry. These complexes are fairly stable in the solid state, and the NMR spectrum of a CDCl_3 solution of the complex $[\text{Rh}\{(R)\text{-1a}\}_2]\text{SbF}_6$ (**8a**) prepared under argon remained unchanged after three days with no other species with a different L/Rh ratio or an unsymmetrical arrangement of the two ligands being observed.

In addition to the expected bis-MonoPhos/Rh complex, a minor byproduct (yield $\leq 5\%$) was formed, regardless of the counterion. If no excess amount of ligand was used in the preparation of the catalyst (2 equiv of **1a** instead of 2.1), its formation could be further minimised. A species that showed the same spectroscopic features of the byproduct was selectively prepared by mixing $[\text{Rh}(\text{nbd})_2]\text{BF}_4$ with 4 equiv of (R) -MonoPhos in dichloromethane at room temperature. Crystals suitable for X-ray analysis were grown that identified the complex as $[\text{Rh}\{(R)\text{-1a}\}_4]\text{BF}_4$ (**9b**).^[19] This is the same species that is formed in much higher amount when the catalyst is prepared from $[\text{Rh}(\text{cod})_2]\text{BF}_4$ and

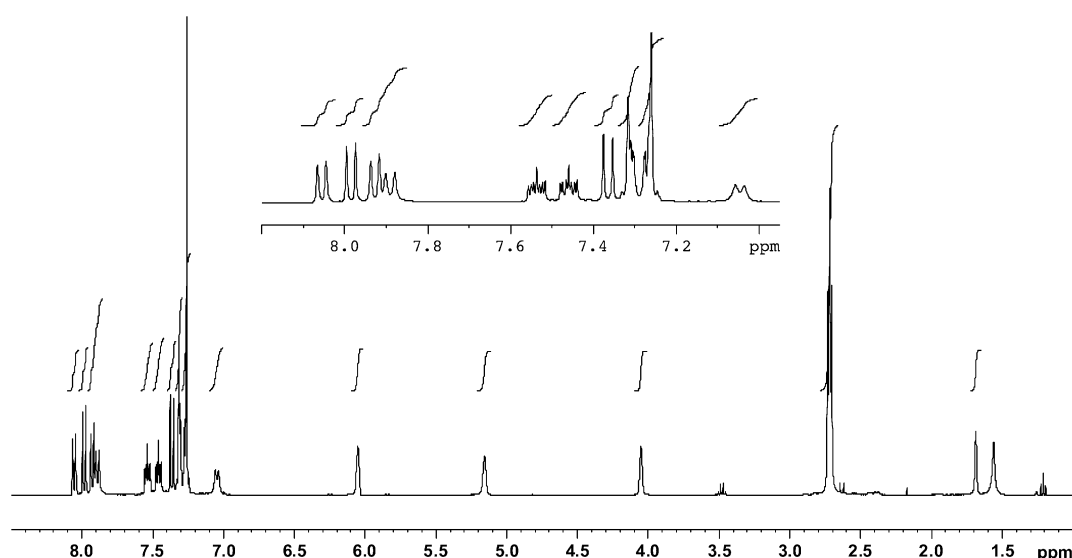
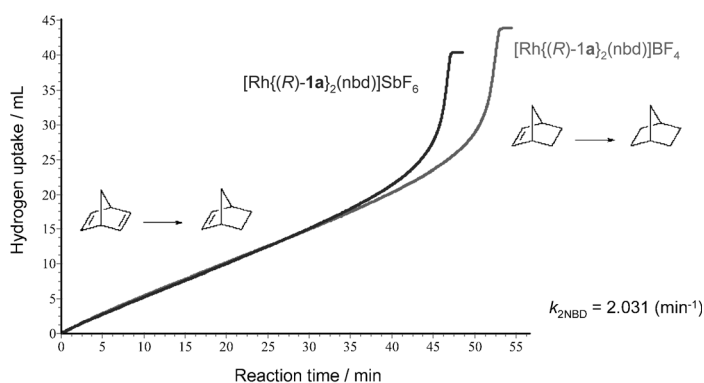


Figure 1. ^1H NMR spectrum of **8a** recorded in CDCl_3 at room temperature.

2.1 equiv of MonoPhos **1a**.^[20] Crystals of **9b** were tested as catalyst in the hydrogenation of test substrate **2a**: in dichloroethane at room temperature under 1 bar total pressure, no conversion of the substrate was observed after 24 h. Therefore **9b** is catalytically inactive under the experimental conditions of the previously reported kinetic investigations. This reinforces the notion that its presence in solution could explain the inverse dependence of the hydrogenation rate on the MonoPhos/Rh ratio:^[11] when the latter is lowered from 2 to 1, the relative amount of the catalytic inactive species **9** formed is reduced and the observed hydrogenation rate increases as it is experimentally observed.^[11]

Kinetic studies: Throughout this study, either complex **8a** or **8b** was used. These complexes are catalyst precursors from which the active catalytic species is generated upon hydrogenation of nbd. The catalytic hydrogenation of nbd in 1,2-dichloroethane^[21] follows the expected behaviour: a clear selectivity for the hydrogenation of the first (nbd to norbornene (nbe)) and the second (nbe to norbornane (nba)) double bond of the diene being observable (Figure 2).^[22] The former is represented by the first linear part of the curve (reaction zero order in the substrate concentration), the latter (faster) by the second part. This effect is quite often found and can be explained with the smaller equilibrium constant of the nbe complex compared to that of the nbd complex (chelate effect), which prevents the complexation of the monoene, a prerequisite for its hydrogenation, as long as there is diene present in solution. The pseudo-first-order rate constant is 2.03 min^{−1} (compare the in situ catalyst [Rh{(S)-**1a**]₂(cod)]BF₄ in *i*PrOH for which a *k*_{obs} of 0.071 min^{−1} has been measured).^[15] Most importantly, the reaction rate is independent of the chosen counterion (BF₄[−] and SbF₆[−]) of the cationic rhodium complexes, because both provide the same intermediates under hydrogenation condi-



[Rh] = 0.01 mmol, nbd = ca. 1 mmol, DCE = 15 mL, 1.01 bar total pressure, 25.0 °C

Figure 2. Hydrogen-consumption curves for the catalytic hydrogenation of norbornadiene promoted by **8a** and **8b**. The difference between the curves in the latter stages of the reactions are due to a slight difference in the amount of diene used in the two experiments.

tions, as probed by NMR spectroscopy and ESI-MS (see the Supporting Information).

Detection of reaction intermediates under hydrogenation conditions

Dimer: When nbd is displaced from the catalyst precursor **8a** by hydrogenation in deuterated CH₂Cl₂ ([Rh] ≡ 0.017 M), the ³¹P NMR spectrum shows that the doublet due to **8a** (d, δ = 138.78 ppm, ¹J(P,Rh) = 251.1; Figure 3a) is no longer present and two sharp doublets of doublets are observed, which is indicative of the formation of a new species that shows two distinct phosphorus resonances that are mutually coupled and also coupled to rhodium (δ = 146.9 ppm, ¹J(P,Rh) = 210 Hz, ¹J(P,P) = 53 Hz; δ = 145.0 ppm, ¹J(P,Rh) = 225 Hz, ¹J(P,P) = 53 Hz) (Figure 3b). Both phosphorus–rhodium coupling constants ¹J(P,Rh) are larger than those of the

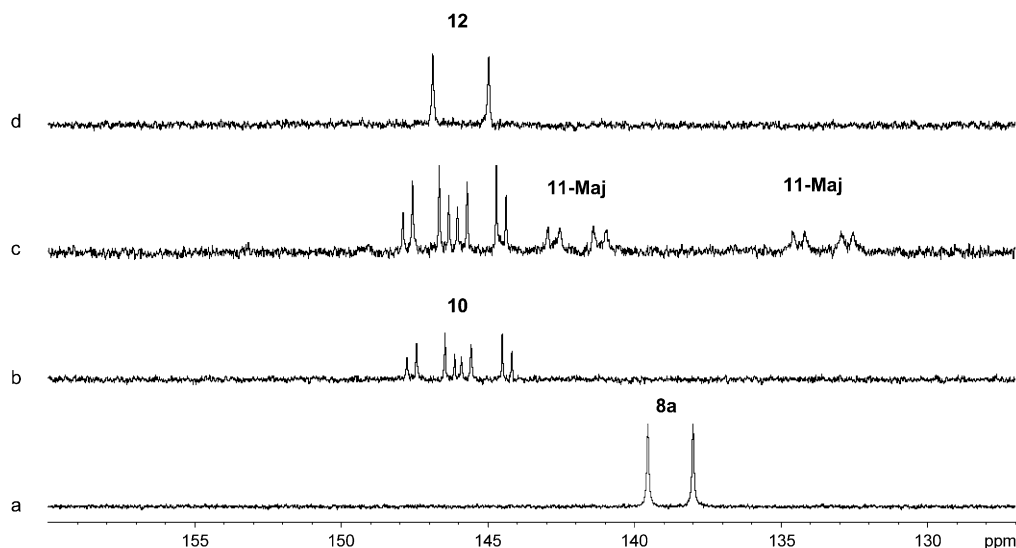


Figure 3. ³¹P NMR spectra of reaction intermediates detected during hydrogenation promoted by **8a** in CD₂Cl₂ at 297 K: a) spectrum of **8a**; b) after hydrogenation for nbd in **8a** is complete; c) after sample degassing from H₂ and the addition of 1.2 equiv of **2a**; d) after complete hydrogenation of **2a**.

catalyst precursor and closely resemble the value found for the η^6 -product complex **12** described later.

In the ^1H NMR spectrum (Figure 4), the appearance of characteristic high-field signals in the region $\delta = 6.0\text{--}7.0$ ppm suggests that an arene fragment of the ligand interacts with the rhodium atom.

To gain more insight into the coordination mode, further analysis of the NMR spectra was accomplished by correlation spectroscopy including both ^1H , ^{103}Rh HMQC and ^{31}P , ^{103}Rh HMQC. A single absorption in the ^{103}Rh NMR spectrum, correlated to both the phosphorus donors, was detected, thus indicating the presence of only one rhodium species.^[23] The chemical shift, $\delta = -620$ ppm (compare with the chemical shift of $\delta = -268$ ppm for **8b**),^[24] is in the range of known values for arene diphosphine Rh complexes.^[25] The observation of cross-peaks in the ^1H , ^{103}Rh HMQC spectrum for the aromatic protons confirmed the coordination

of the “outer” ring of the naphthyl group (see the Supporting Information).^[26]

By analogy with previously reported species for both Rh–diphosphines and Rh–monophosphine complexes, it is concluded that a dimeric species **10** (Scheme 5) has formed upon hydrogenation of nbd in the catalyst precursor.^[12,27] The dimeric formulation was further supported by ESI-MS: besides a small peak at m/z 1878.7 due to $[(\text{Rh}\{(R)\text{-1a}\}_2)_2]-(\text{SbF}_6)^+$, the base peak is observed at 821.6, this value being obtained by dividing the molecular mass of the dimer cation $[(\text{Rh}\{(R)\text{-1a}\}_2)_2]^{2+}$ by its double charge (Table 3). The

Table 3. Selected ESI-MS results for **8a** and **10**.

Compound	Fragment	[M]	z	m/z
8a	$[\text{Rh}\{(R)\text{-1a}\}_2]^+$	821	1	821
10	$[\text{Rh}\{(R)\text{-1a}\}_2]^{2+}$	1643	2	821.5

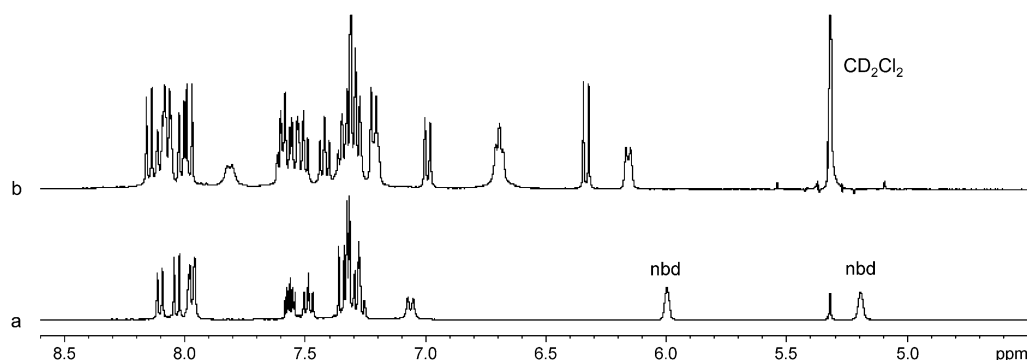
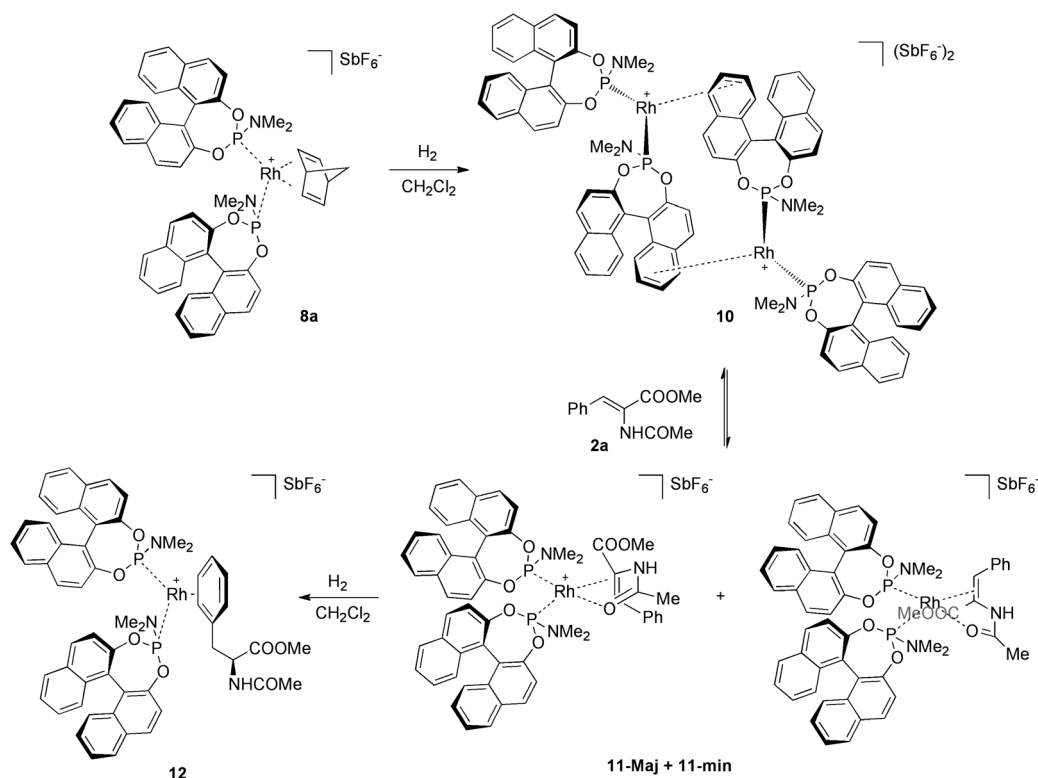


Figure 4. Comparison between the low-field portion of the ^1H NMR spectrum of a) **8a** and b) that of **10** in deuterated CH_2Cl_2 .



Scheme 5. Intermediates detected during hydrogenation promoted by **8a**.

isotopic peak patterns at m/z 821–814 shown in Figure 5 allow us to discriminate between the cationic fragment $[\text{Rh}\{(R)\text{-1a}\}_2]^+$ derived from the catalyst precursor **8a** and

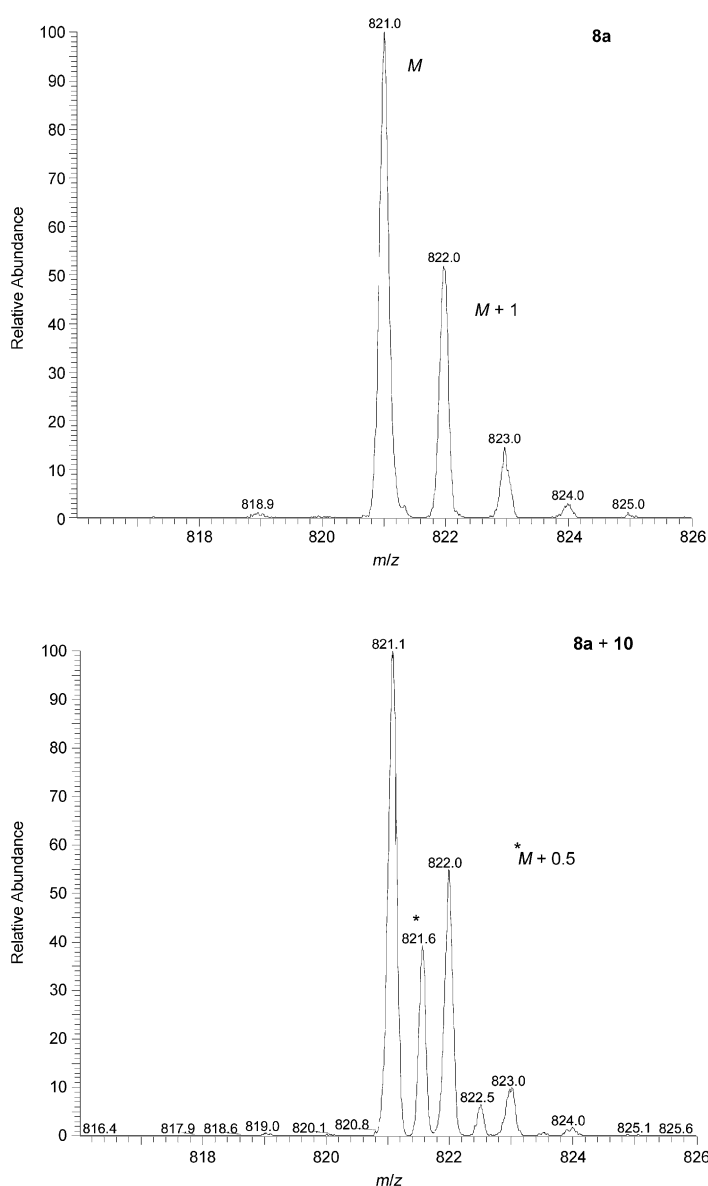


Figure 5. Isotopic cluster of the m/z 821.1 peak of species **8a** (top spectrum) and superimposition of the isotopic cluster of the m/z 821.1 peak of species **8a** and the isotopic cluster of the m/z 821.6 peak of species **10** (bottom spectrum).

that derived from the dimer **10**: because the dimer is doubly charged, its $M+1$ peak shows up as a $M+0.5$ peak, which is missing in the isotopic pattern of the m/z 821.1 peak due to the $[\text{Rh}\{(R)\text{-1a}\}_2]^+$ fragment derived from the catalyst precursor.

In the dimer, the phosphorus atoms that bear the bridging naphthyls are chiral, which means that in principle different diastereomeric dimers may exist.^[27e,f] However, within the

limits of the sensitivity of the instrument, only one species was observed in our case at room temperature.

The dimer is very stable in CH_2Cl_2 within the 0.0174–0.0043 M concentration range with no indication of the formation of solvato species upon dilution.^[28] Nor were hydride complexes detected in the solutions of the dimer under hydrogen (1 bar total pressure) at room temperature. That is, no signals were detected in the ^1H NMR spectrum at high field, beyond $\delta=0$ up to -30 ppm.^[29–31]

Rh–substrate adducts: The prochiral substrate, methyl (*Z*)-2-acetamidocinnamate (**2a**), is known to form strong chelate complexes when treated with various $[\text{Rh}(\text{diphosphine})(\text{S})_2]^+$ ($\text{S} = \text{solvent}$).^[1b,14a,d,27d,32] When a 1.2-fold excess amount of mac was added to an argon-blanketed solution ($[\text{Rh}] = 0.017$ M) of the dimer **10** at room temperature, new signals, besides those of the dimer, appeared in the ^{31}P NMR spectrum (Figure 3c). The new signals are broad, yet their multiplicity is consistent with the formation of a catalyst–substrate adduct $[\text{Rh}\{(R)\text{-1a}\}_2(\text{mac})]\text{SbF}_6$ (**11**). Under these conditions, however, the formation of **11** is slow and a gentle heating of the sample was useful for speeding up the reaction. The variable-temperature spectra of **11** were run on a more concentrated solution of the dimer ($[\text{Rh}] = 0.025$ M) that was gently heated until NMR spectroscopic monitoring at room temperature showed that the ratio between **10** and **11** was as high as 1:3 (Figure 6a–d).

By lowering the temperature, the signals broaden further and almost disappear in the background at 263 K due to an intense exchange. Decreasing the temperature further to 221 K, a second set of signals with a similar eight line pattern appears at lower field: the two sets of signals are well resolved and the following parameters are measured: **11-Maj** $\delta = 133.0$ ppm (dd, $^1J(\text{P,Rh}) = 265$ Hz, $^2J(\text{P,P}) = 62$ Hz); $\delta = 141.1$ ppm (dd, $^1J(\text{P,Rh}) = 254$ Hz, $^2J(\text{P,P}) = 62$ Hz); **11-min** $\delta = 136.9$ ppm (dd, $^1J(\text{P,Rh}) = 257$ Hz, $^2J(\text{P,P}) = 69$ Hz); $\delta = 148.7$ ppm (dd, $^1J(\text{P,Rh}) = 242$ Hz, $^2J(\text{P,P}) = 69$ Hz). At 221 K the two species are present in approximately a 3-to-2 ratio. The observed line patterns and coupling constants $^1J(\text{P,Rh})$ and $^2J(\text{P,P})$ are similar to those observed in related complexes in which it has been demonstrated that both the C=C bond, either through the *si* or *re* face, and the oxygen of the amido group are coordinated to rhodium in a chelate fashion and are therefore ascribed to species **11-Maj** and **11-min** (Scheme 5). The occurrence of the chelate coordination of mac is further supported by ^{103}Rh NMR spectroscopic evidence (vide infra) and by the characteristic chemical shift of the coordinated olefinic $=\text{CH}-$ (see Figure SI20 in the Supporting Information).

This coordination mode renders the two MonoPhos ligands non-equivalent, thus giving rise to two distinct phosphorus resonances that are mutually coupled and also coupled to rhodium.^[33] The formation of the catalyst–substrate adducts was further corroborated by the ESI-MS spectra in which the corresponding molecular ion peak is clearly visible (see the Supporting Information). It is not possible to

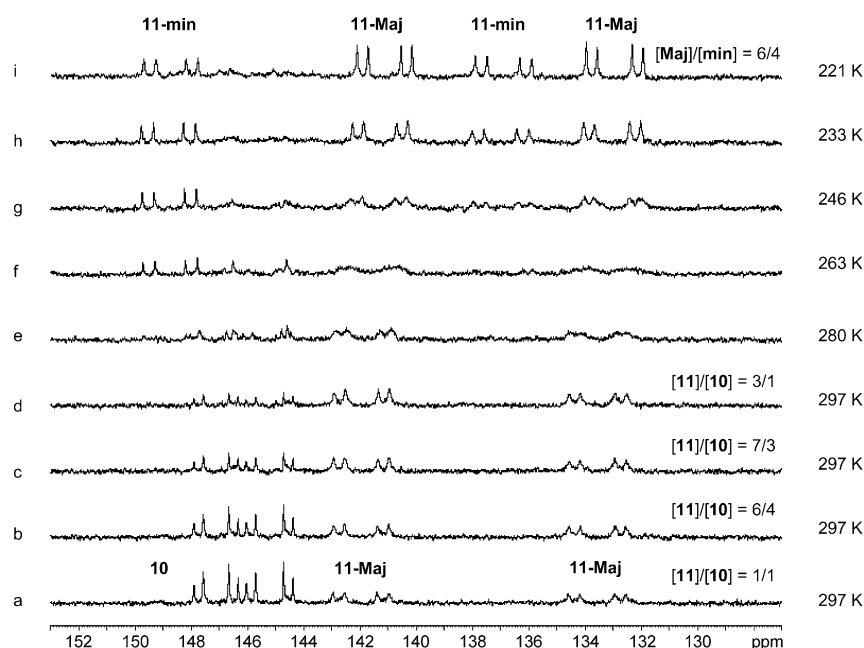


Figure 6. Variable-temperature ^{31}P NMR spectra of adducts **11** in deuterated CH_2Cl_2 . Spectra (b–d) have been recorded after having warmed up the samples to favour formation of **11** from dimer **10**.

say why the minor isomer is not observable at room temperature. It can either be present in very low concentration or its signal may be too broad due to extensive line broadening. The two diastereomers are in dynamic equilibrium and their signals show a different line broadening with increasing temperature, which might be attributed to a different dissociation rate.

Although at 221 K the ^{31}P NMR spectrum of the adducts **11** is well resolved, the corresponding ^1H NMR spectrum is ill-defined due to the presence of the dimer **10** and free mac. This hampered any attempt to clear their stereochemistry and to correlate their absolute configuration with that of the prevailing hydrogenation product enantiomer. Elucidation of the dynamic processes by either ^1H or ^{31}P exchange spectroscopy at 221 K proved unsuccessful.^[34] However, it became evident that the ratio between major and minor diastereomers changed immediately upon temperature variation (see Figure SI19 in the Supporting Information). Because of this fast interconversion, hydrogenation at low temperature to assess which of the two adducts is preferentially reduced to afford the prevailing enantiomer and whether the hydrogenation does or does not follow the Halpern mechanism was not attempted because its result would have been inconclusive and even misleading.

The 2D (^{31}P , $^{103}\text{Rh}\{^1\text{H}\}$) correlation spectrum of the two adducts at 221 K shows that the $\delta(^{103}\text{Rh})$ of the major diastereomer appears at $\delta = 324$ ppm, at lower frequency (more shielded) than the chemical shift $\delta(^{103}\text{Rh})$ of the minor diastereomer, $\delta = 617$ ppm, thereby reflecting an electronic difference at rhodium between the two species (Figure 7). The very same trend had been observed for the analogous rhodium complexes that contain the chiral diphosphines (*S,S*)-

chiraphos and (*S,S*)-dipamp,^[35] for which it is well established that the minor adduct is the more reactive toward hydrogen oxidative addition. According to von Philipsborn, the difference in $\delta(^{103}\text{Rh})$ chemical shift between the two diastereomers is influenced by, among several factors, the size of the metal valence orbitals, $\langle r^{-3} \rangle$, and this factor decreases (r increases) for the major diastereomer because of a better overlap between ligand and metal-based valence orbitals. Because of the negative sign of the paramagnetic shielding term σ_p , this implies a shift to lower frequency. The increasing shielding of the metal should therefore indicate stronger binding of the substrate, which in turn would render the metal less reactive

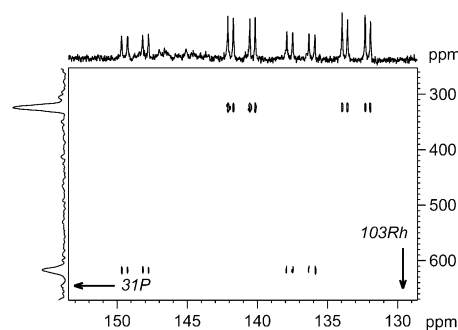


Figure 7. 2D (^{31}P , $^{103}\text{Rh}\{^1\text{H}\}$) HMQC NMR spectrum (162.0 MHz) of adducts **11** in deuterated CH_2Cl_2 recorded at 221 K. Chemical shifts $\delta(^{103}\text{Rh})$ **11-Maj** = 324 ppm ($\Xi = 3.161025$ MHz); **11-min** = 617 ppm ($\Xi = 3.161951$ MHz).

toward adding another ligand such as hydrogen gas. This would suggest that it is the minor diastereomer of the two substrate complexes that is the more reactive one and that leads to the product.

The relative stability of the dimer **10** with respect to the catalyst-substrate adducts might explain the unexpected kinetic behaviour observed in the catalytic reduction of mac with **8a**. Two experiments directed towards hydrogen consumption measurements have been run (see Figure SI70 in the Supporting Information): in the first experiment, the catalyst precursor was prehydrogenated (induction period) to reduce nbd. Methyl (*Z*)-2-acetamidocinnamate was then added and hydrogen consumption was monitored until complete conversion of the substrate. In this case, the measured rate should reflect the “intrinsic activity” of the catalyst as it relates to mac hydrogenation, with no influence of the in-

duction period necessary to displace nbd. In the second experiment, no catalyst prehydrogenation was performed. All reagents were placed in the reaction vessel and hydrogen-consumption monitoring was started immediately after hydrogen gas was admitted into the reactor. Surprisingly, the reaction rate was faster in this latter case, contrary to what normally observed with similar rhodium-catalyst-containing diphosphines.^[22] One possible explanation might be the formation of the dimer when prehydrogenation of the catalyst is carried out in the absence of mac. The lower rate of mac hydrogenation observed in this case might then reflect the slow formation of the catalyst–substrate adducts **11** from the dimer **10**.

Rh–product adducts: Hydrogenation of the solution that contained the catalyst–substrate adducts **11-Maj** and **11-min** (1 bar total pressure) at room temperature provided the expected product *N*-acetylphenylalanine methyl ester (*S*)-mac(H)₂ in 93% *ee*, in accordance with published data.^[11] The ³¹P NMR spectrum of the solution showed a doublet at $\delta = 145.9$ ppm with $^1J(\text{P,Rh}) = 308$ Hz (Figure 3d), and in the ESI mass spectrum a peak at *m/z* 1041.9, which is supportive of the presence of a catalyst–product adduct [Rh{(R)-**1a**}_2[(*S*)-mac(H)₂]]SbF₆ (**12**), was observed. The product is likely coordinated to rhodium through the phenyl ring as suggested by the appearance of up-field resonances in the ¹H NMR spectrum between $\delta = 6$ and 7 ppm (Figure 8). Further characterisation has been achieved both in dichloromethane and 1,2-dichloroethane solutions (see Figures SI22–SI25 in the Supporting Information).

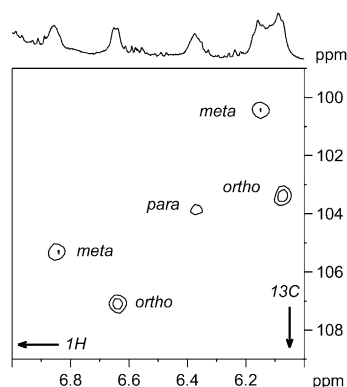


Figure 8. Section of the ¹H,¹³C HMQC NMR spectrum of the hydrogenation solution of mac/[Rh{(R)-**1a**}_2(nbd)]SbF₆, molar ratio 1.2, in [D₄]1,2-dichloroethane taken after complete conversion of mac. The signals of the η⁶-coordinated reaction product in complex **12** are shown.

Complex **12** is coordinatively labile. At an Rh/product ratio of 0.8, only half of the arene is coordinated and the exchange with the free product is detectable on the NMR spectroscopic timescale. The nature of the remaining Rh complexes was not established (due to strong line broadening, no other species were visible in the ³¹P NMR spectrum), but the presence of the dinuclear complex **10** is most likely.

The ¹⁰³Rh chemical shift $\delta(^{103}\text{Rh})$ at –849 ppm is then typical of an η⁶-arene Rh species.^[25] A similar product–catalyst adduct had been observed in the hydrogenation of mac with a rhodium complex of (*S,S*)-1,2-bis(*tert*-butylmethylphosphino)ethane.^[36]

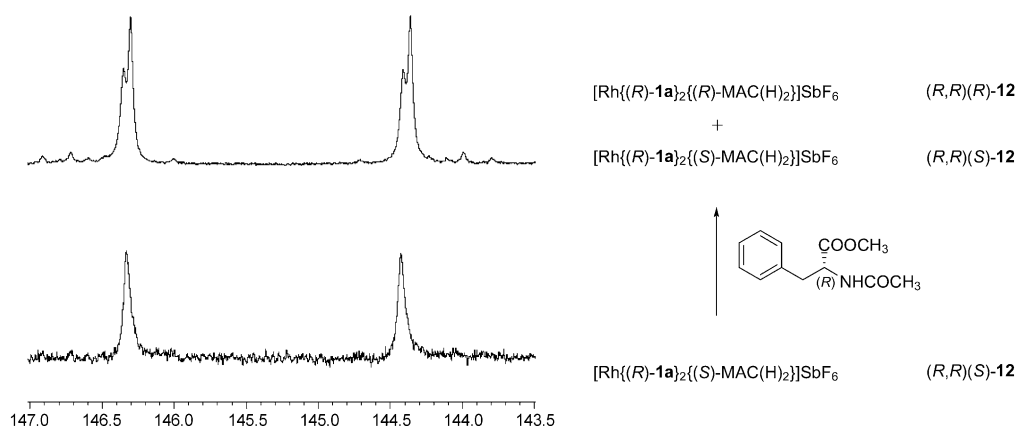
That the observed doublet in the ³¹P NMR spectrum is truly due to the catalyst–product adduct could be confirmed by the following experiment. When the hydrogenation of mac is carried out with [Rh{(R)-**1a**}_2(nbd)]SbF₆, the configuration of the prevailing enantiomer of the hydrogenated product *N*-acetylphenylalanine methyl ester is *S*. Upon addition of 1.2 equiv of the other enantiomer (*R*)-*N*-acetylphenylalanine methyl ester to the above solution, a second doublet appeared in the ³¹P NMR spectrum with a chemical shift and a coupling constant ($\delta = 145.38$ ppm (d, $^1J(\text{P,Rh}) = 308.0$ Hz)) very similar to those of the first one (Scheme 6). The new doublet is therefore attributed to the diastereomeric “catalyst–product” adduct (*R,R*)(*R*)-**12**. The same results were obtained in separate experiments in which the catalyst–product adducts were prepared by hydrogenation of **8a** in the presence of *N*-acetyl-*rac*-phenylalanine methyl ester, *N*-acetyl-(*R*)-phenylalanine methyl ester and *N*-acetyl-(*S*)-phenylalanine methyl ester, respectively. The difference in the chemical shift of the two diastereomeric adducts, approximately $\delta = 0.5$ ppm, is in line with what previously observed for analogous diastereomeric adducts between {Rh[(*S,S*)-bdpp](CD₃OD)₂]ClO₄ (bdpp = 2,4-bis-diphenylphosphino)pentane) and *N*-acetyl-(*R*)-phenylalanine and *N*-acetyl-(*S*)-phenylalanine.^[37] (³¹P and ¹⁰³Rh NMR spectroscopic data of all detected species are collected in Table 4).

The coordinated product can be very easily displaced from the catalyst by addition of fresh mac. Five equivalents are sufficient to shift the equilibrium completely in favour of the catalyst–substrate adducts **11** as confirmed by the ESI-MS spectrum of the solution in which only the peak relative to **11** is present (see Figures SI66–SI68 in the Supporting Information).

Hydrogenation of a 200-fold excess amount of mac with the same solution (final rhodium concentration [Rh] = 0.0004 M) at room temperature provided the product *N*-acetyl-(*R*)-phenylalanine methyl ester of the same optical purity (93% *ee*) as in the stoichiometric hydrogenation.

Conclusion

In this study, we have been able to observe and characterise several Rh–phosphoramidite species involved in the asymmetric hydrogenation of methyl (*Z*)-2-acetamidocinnamate (**2a**). First of all, the pre-catalyst [Rh{(R)-MonoPhos}_2(nbd)]X **8** (with X being either BF₄[–], SbF₆[–], PF₆[–] or CF₃SO₃[–]), was synthesised and characterised by means of NMR spectroscopy and ESI-MS. Upon hydrogenation of the catalyst precursor **8a** (X = SbF₆[–]), a new dimeric species **10** was formed. In this species, the monodentate phosphoramidite now plays the role of a bidentate bridging ligand and can coordinate a second unsaturated Rh center through one



Scheme 6. ^{31}P NMR spectra (CD_2Cl_2 , 297 K) of catalyst–product adduct $(R,R)(S)\text{-12}$ (bottom) and of a mixture of $(R,R)(S)\text{-12}$ and $(R,R)(R)\text{-12}$ (top).

Table 4. Summary of ^{31}P and ^{103}Rh NMR spectroscopy data recorded in $[\text{D}_2]\text{CH}_2\text{Cl}_2$ for the hydrogenation intermediates reported in this study.

Compound	Multiplet	$\delta(^{31}\text{P})$ [ppm]	$J(\text{P,Rh})$ [Hz]	$J(\text{P,P})$ [Hz]	$\delta(^{103}\text{Rh})$ [ppm]
8a	d	138.9	253.1	–	(–268) ^[a]
10	dd	145.0	224.6	53.0	–620
11-Maj	dd	146.9	209.8	53.0	–620
	dd	133.0	265.0	63.0	324
11-min	dd	141.1	254.0	62.0	324
	dd	136.9	257.0	69.0	617
	dd	148.7	242.0	69.0	617
$(R,R)(S)\text{-12}$	d	145.9	308.0	–	–849
$(R,R)(R)\text{-12}$	d	145.3	308.0	–	–849

[a] This value refers to complex **8b**.

of its naphthyl groups. The dimer is very stable in CH_2Cl_2 within the 0.0174–0.0043 M concentration range with no indication as to the formation of solvate species upon dilution. No hydride complexes were detected in the solutions of the dimer under hydrogen. This is most probably due to the high π -acidic character of the MonoPhos ligands, which consequently fails to stabilise the octahedral dihydride Rh^{III} complex.^[38]

The addition of mac **2a** to the dimeric Rh species led to the formation of two diastereomeric catalyst–substrate adducts $[\text{Rh}\{(\text{R})\text{-MonoPhos}\}_2(\text{mac})]\text{SbF}_6$ (**11-Maj** and **11-min**), which were detected and characterised by NMR spectroscopy and ESI-MS. The NMR spectra show that two molecules of MonoPhos are coordinated to rhodium in these crucial hydrogenation intermediates. The occurrence of chelate coordination of mac in the adducts **11** can be deduced from the shift at higher field of the olefinic $=\text{CH}-$ resonance and, even more conclusively, from the rhodium chemical shifts that are as expected for such a type of chelate complexes.

Addition of H_2 to this catalyst–substrate adduct leads to the formation of the hydrogenated product with the expected *ee* value (93 %) and configuration (*S*). The hydrogenated product remains bound to the metal in a new Rh-product adduct **12** from which it can be promptly displaced upon addition of fresh mac. Consequently, we have demonstrated that different Rh species, all of which bear two ligands per

Rh, can be responsible for all the catalytic steps involved in the hydrogenation. In addition to previous results (the hetero-combination of ligand, the presence of non-linear effects), this study provides conclusive evidence that the active species in Rh/phosphoramidite contains two monodentate ligands.

From the ^{103}Rh NMR spectrum, the minor adduct **11-min** turns out to be the most kinetically labile of the two diastereoisomers. This fact supports the conclusion that the absence of visible NMR peaks in the room temperature ^1H NMR spectrum of this species is caused by an intense exchange rather than to a concentration effect. Since according to Gridnev^[1b] the catalyst–substrate complex that exchanges more intensively is the one that is hydrogenated at a faster rate, this behaviour is indicative that the relative ease of the hydrogenation of **11-Maj** and **11-min** should be in favour of the minor adduct **11-min**.

In summary, although it was not possible to assess by direct methods the exact stereochemistry of the two Rh–substrate diastereomers, from these arguments we can confidently conclude that the major adduct **11-Maj** may be the less reactive towards the activation of H_2 . In which case, the Rh/phosphoramidite system would follow an anti lock and key mechanism, opposite to the one claimed for the similar Rh/phosphite system.^[8] Nevertheless, further studies are needed to clarify this last point for certain.

Experimental Section

All manipulations involving air- and moisture-sensitive organometallic compounds were carried out using standard Schlenk techniques under argon atmosphere. Dichloromethane and 1,2-dichloroethane were freshly distilled from calcium hydride, diethyl ether and *n*-hexane from sodium benzophenone ketyl. Deuterated dichloromethane $[\text{D}_2]\text{CH}_2\text{Cl}_2$ and 1,2-dichloroethane $[\text{D}_4]\text{DCE}$ used for the detection of intermediates under hydrogenation conditions were distilled from calcium hydride. Solutions of crude reaction mixtures were filtered when necessary through a short pad of filter aid Fluka Celite 535. Catalyst precursors $[\text{Rh}(\text{nbd})\text{Cl}]_2$ ^[39] and $[\text{Rh}(\text{nbd})_2]\text{X}$ ^[40] (X^- being either SbF_6^- , BF_4^- , PF_6^- or CF_3SO_3^-) were prepared according to published procedures. NMR spectra were recorded using Varian Mercury Plus (400 MHz for ^1H), Bruker AV-300 (300 MHz

for ^1H) and Bruker AV-400 (400 MHz for ^1H) spectrometers. Chemical shifts δ are reported in ppm relative to 85% H_3PO_4 for ^{31}P and the solvent resonance for ^1H and ^{103}Rh chemical shifts are given relative to $\Xi(^{103}\text{Rh})=3.16$ MHz. Coupling constants, J , are given in Hz. Mass spectrometric analyses were performed using an LCQ Deca XP ion trap MS (ThermoFisher, Bremen, Germany).

Standard procedure for the preparation of complexes 8: A solution of (*R*)-MonoPhos (0.36 mmol, 2.1 equiv) in freshly distilled THF or CH_2Cl_2 (8 mL) was added dropwise to a stirred solution of $[\text{Rh}(\text{nbd})_2]\text{X}$ (0.27 mmol) in freshly distilled THF or CH_2Cl_2 (2 mL). The mixture was stirred at room temperature for 2 h. It was then concentrated under reduced pressure and the complex precipitated by addition of diethyl ether. The solid was repeatedly washed with diethyl ether and then dried in vacuum to give the complex as an orange-yellow solid. All complexes show similar ^1H , ^{13}C and ^{31}P NMR spectra. ^1H and ^{13}C NMR chemical shifts are reported only for $[\text{Rh}(\text{nbd})](\text{R})\text{-MonoPhos}_2[\text{BF}_4]$ in CDCl_3 and CD_2Cl_2 (for the latter solvent, see Table SI1 in the Supporting Information).

Complex 8a: Isolated yield: 89%. ^{31}P NMR (161.89 MHz, CDCl_3 , 298 K): $\delta=138.30$ ppm (d, $^1J(\text{P,Rh})=252.0$ Hz); ESI-MS: m/z (%): 913 (84) $[\text{Rh}(\text{nbd})](\text{R})\text{-MonoPhos}_2]^+$, 821 (12) $[\text{Rh}(\text{R})\text{-MonoPhos}_2]^+$, 554 (100) $[\text{Rh}(\text{nbd})](\text{R})\text{-MonoPhos}]^+$, 234.9 (100) (SbF_6^-) , 236.9 (75) (SbF_6^-) .

Complex 8b: This complex was prepared in CH_2Cl_2 . Isolated yield: 89%. ^1H NMR (400 MHz, CDCl_3 , 298 K): $\delta=1.71$ (brs, 2H; $-\text{CH}_2-\text{nbd}$), 2.73 and 2.74 (overlapping d, $^3J(\text{H,P})=5.4$ Hz, 12H; $-\text{NCH}_3$), 4.11 (brs, 2H; $-\text{CH}=\text{CH}=\text{nbd}$), 5.25 (brs, 2H; $-\text{CH}=\text{CH}=\text{nbd}$), 6.09 (brs, 2H; $-\text{CH}=\text{CH}=\text{nbd}$), 7.00 (brd, 2H; H_{Ar} , $J=7.3$ Hz), 7.24–7.27 (m, 4H; H_{Ar}), 7.29–7.33 (m, 4H; H_{Ar}), 7.38 (d, $J=8.8$ Hz, 2H; H_{Ar}), 7.44 and 7.46 (overlapping dd, $^1J=5.4$ Hz, $^2J=2.4$ Hz; 1H; H_{Ar} and $^1J=5.8$ Hz, $^2J=2.9$ Hz, 1H; H_{Ar}), 7.52 and 7.54 (overlapping dd, $^1J=5.4$ Hz, $^2J=2.4$ Hz; 1H; H_{Ar} and $^1J=5.4$ Hz, $^2J=2.4$ Hz, 1H; H_{Ar}), 7.86 (d, $J=8.8$ Hz, 2H; H_{Ar}), 7.92 (d, $J=8.3$ Hz, 2H; H_{Ar}), 7.98 (d, $J=8.8$ Hz, 2H; H_{Ar}), 8.05 ppm (d, $J=8.3$ Hz, 2H; H_{Ar}); ^{13}C NMR (100.56 MHz, CDCl_3 , 298 K): $\delta=38.05$ and 38.10 (overlapping d, $J(\text{C,P})=5.4$ Hz, 2C; $-\text{NCH}_3$ and $J(\text{C,P})=6.1$ Hz, 2C; $-\text{NCH}_3$), 55.47 (s, 1C; $-\text{CH}_2-\text{nbd}$), 72.20 (brs, 2C; $-\text{CH}=\text{CH}=\text{nbd}$), 93.36 (brs, 2C; $-\text{CH}=\text{CH}=\text{nbd}$), 120.94 (s, 2C; C_{Ar}), 121.07 (s, 2C; C_{Ar}), 122.48 (s, 2C; C_{Ar}), 123.13 (s, 2C; C_{Ar}), 125.99 (s, 2C; C_{Ar}), 126.26 (s, 2C; C_{Ar}), 126.95 (s, 2C; C_{Ar}), 127.15 (s, 2C; C_{Ar}), 127.26 (s, 2C; C_{Ar}), 127.50 (s, 2C; C_{Ar}), 127.58 (s, 2C; C_{Ar}), 128.82 (s, 2C; C_{Ar}), 128.96 (s, 2C; C_{Ar}), 130.97 (s, 2C; C_{Ar}), 131.69 (s, 2C; C_{Ar}), 131.78 (s, 2C; C_{Ar}), 131.91 (s, 2C; C_{Ar}), 132.57 (s, 2C; C_{Ar}), 147.93 (brs, 2C; C_{Ar}), 148.74 ppm (brs, 2C; C_{Ar}); ^{31}P NMR (161.89 MHz, CDCl_3 , 298 K): $\delta=138.70$ ppm (d, $^1J(\text{P,Rh})=250.8$ Hz); ^{103}Rh NMR (12.6 MHz, $[\text{D}_2]\text{CH}_2\text{Cl}_2$, 297 K): $\delta=-268$ ppm; ESI-MS: m/z (%): 913 (84) $[\text{Rh}(\text{nbd})](\text{R})\text{-MonoPhos}_2]^+$, 821 (12) $[\text{Rh}(\text{R})\text{-MonoPhos}_2]^+$, 554 (100) $[\text{Rh}(\text{nbd})](\text{R})\text{-MonoPhos}]^+$; 87 (100) (BF_4^-) , 86 (24.8) (BF_4^-) .

Complex 8c: Isolated yield: 88%. ^{31}P NMR (161.89 MHz, CDCl_3 , 298 K): $\delta=138.70$ (d, $^1J(\text{P,Rh})=251.8$ Hz), -144.13 ppm ($J(\text{P,F})=712.6$ Hz); ESI-MS: m/z (%): 913 (84) $[\text{Rh}(\text{nbd})](\text{R})\text{-MonoPhos}_2]^+$, 821 (12) $[\text{Rh}(\text{R})\text{-MonoPhos}_2]^+$, 554 (100) $[\text{Rh}(\text{nbd})](\text{R})\text{-MonoPhos}]^+$; 144.9 (100) (PF_6^-) .

Complex 8d: Isolated yield: 86%. ^{31}P NMR (161.89 MHz, CDCl_3 , 298 K): $\delta=138.69$ ppm (d, $^1J(\text{P,Rh})=250.8$ Hz); ESI-MS: m/z (%): 913 (84) $[\text{Rh}(\text{nbd})](\text{R})\text{-MonoPhos}_2]^+$, 821 (12) $[\text{Rh}(\text{R})\text{-MonoPhos}_2]^+$, 554 (100) $[\text{Rh}(\text{nbd})](\text{R})\text{-MonoPhos}]^+$; 149 (100) $(\text{CF}_3\text{SO}_3^-)$.

Complex 9b: $[\text{Rh}(\text{nbd})_2]\text{BF}_4$ (35 mg, 0.093 mmol) and (*R*)-MonoPhos (138 mg, 0.38 mmol, 4.1 equiv) were placed in a Schlenk flask. Freshly distilled dichloromethane (10 mL) was added to give a clear yellow solution, which was stirred for 2 h at room temperature. The solution was concentrated under reduced pressure and the product precipitated by addition of *n*-hexane. The solid was repeatedly washed with *n*-hexane and then dried in vacuum to give the complex as a light yellow solid. Isolated yield: 130 mg, 85%. Crystals suitable for X-ray analysis were obtained by recrystallisation from dichloroethane/*n*-hexane. The X-ray investigation confirmed the structure already published.^[11] NMR spectroscopy data were collected on a solution of the recrystallised sample: no attempt was made to interpret the rather complicated ^{31}P NMR spectrum (see Figures

SI14 and SI15 in the Supporting Information). ESI-MS (HRMS, positive ion mode): m/z calcd for $\text{C}_{88}\text{H}_{72}\text{N}_4\text{O}_8\text{P}_4\text{Rh}$: 1539.335 $[M^+]$; found: 1539.3391.

Detection of reaction intermediates under hydrogenation conditions

Complex 10: A solution of **8a** (20 mg, 0.017 mmol) in CD_2Cl_2 (1 mL) was prepared in a 5 mm YOUNG NMR spectroscopy tube under argon. H_2 gas ($p=1$ bar) was then admitted into the sample, which was intensively shaken manually until hydrogenation at room temperature of coordinated nbd was complete. During the course of the hydrogenation, the solution turned intensively dark red. ^1H and ^{31}P NMR spectra were recorded before and after degassing the sample from hydrogen. No signals relative to hydride species were detected. ^{31}P NMR (161.89 MHz, $[\text{D}_2]\text{CH}_2\text{Cl}_2$, 298 K): $\delta=145.05$ (dd, $^1J(\text{P,Rh})=224.6$ Hz, $J(\text{P,P})=52.6$ Hz), 146.95 ppm (dd, $^1J(\text{P,Rh})=209.8$ Hz, $J(\text{P,P})=53.3$ Hz); ^{103}Rh NMR (12.6 MHz, $[\text{D}_2]\text{CH}_2\text{Cl}_2$, 297 K): $\delta=-620$ ppm; ESI-MS (positive ion mode): m/z (%): 1878.7 (14) $([\text{Rh}(\text{R})\text{-MonoPhos}_2](\text{SbF}_6))^+$, 821.1 (100) $([\text{Rh}(\text{R})\text{-MonoPhos}_2])^+$.

Complexes 11-Maj and 11-min: After removal of hydrogen through three consequent cycles of freezing, pumping and warming, (*Z*)-2-acetamidocinnamic methyl ester **2a** (mac, 4.6 mg, 0.021 mmol, 1.2 equiv) was added to the above prepared sample under argon. The sample was shaken manually and gently warmed to speed up formation of the catalyst substrate adducts. ^{31}P NMR (400 MHz, $[\text{D}_2]\text{CH}_2\text{Cl}_2$, 218 K): **11-Maj** $\delta=133.0$ (dd, $^1J(\text{P,Rh})=265.0$ Hz, $J(\text{P,P})=63.0$ Hz), 141.1 ppm (dd, $^1J(\text{P,Rh})=254.0$ Hz, $J(\text{P,P})=62.0$ Hz); **11-min** $\delta=136.9$ (dd, $^1J(\text{P,Rh})=257.0$ Hz, $J(\text{P,P})=69.0$ Hz), 148.7 ppm (dd, $^1J(\text{P,Rh})=242.0$ Hz, $J(\text{P,P})=69.0$ Hz); ^{103}Rh NMR (12.6 MHz, $[\text{D}_2]\text{CH}_2\text{Cl}_2$, 183 K): **11-Maj** $\delta=324$ ppm; **11-min** $\delta=617$ ppm; ESI-MS (positive ion mode): m/z (%): 1039.9 (22) $([\text{Rh}(\text{R})\text{-MonoPhos}_2](\text{mac}))^+$, 821.1 (100) $([\text{Rh}(\text{R})\text{-MonoPhos}_2])^+$.

Complex (R,R)(S)-12: The above sample was degassed from argon by three consequent cycles of freezing, pumping and warming. H_2 gas ($P=1$ bar) was then admitted into the sample, which was intensively shaken until NMR spectroscopy showed hydrogenation of mac to *N*-acetylphenylalanine methyl ester mac(H)₂ was complete. ^{31}P NMR (400 MHz, $[\text{D}_2]\text{CH}_2\text{Cl}_2$, 298 K): $\delta=145.9$ ppm (d, $^1J(\text{P,Rh})=308.0$ Hz); ^{103}Rh NMR (12.6 MHz, $[\text{D}_2]\text{CH}_2\text{Cl}_2$, 297 K): $\delta=-849$ ppm; ESI-MS: m/z (%): 1041.9 (60) $([\text{Rh}^+(\text{R})\text{-MonoPhos}_2](\text{macH}_2))^+$, 821.1 (100) $([\text{Rh}(\text{R})\text{-MonoPhos}_2])^+$. GC analysis of this sample shows that it contains (*S*)-*N*-acetylphenylalanine methyl ester in 93% *ee*.

NMR spectra, ESI-MS analyses, GC chromatograms and hydrogen consumption curves are to be found in the Supporting Information.

Acknowledgements

Collaborative research carried out by S.G. and E.A. within the framework of the COST D40 EU project. E.A. acknowledges partial financial support from the Regione Autonoma della Sardegna, L.R. 7 Agosto 2007, n. 7. The skilful technical assistance of Cornelia Prippenow of the Leibniz-Institut für Katalyse e.V. an der Universität Rostock in running hydrogen-consumption measurements is gratefully acknowledged.

- [1] a) *Handbook of Homogeneous Hydrogenation*, (Eds.: J. G. de Vries, C. J. Elsevier), Wiley-VCH, Weinheim, 2007; b) I. D. Gridnev, T. Imamoto, *Chem. Commun.* 2009, 7447–7464, and references therein.
- [2] a) F. Lagasse, H. B. Kagan, *Chem. Pharm. Bull.* 2000, 48, 315–324; b) I. V. Komarov, A. Börner, *Angew. Chem.* 2001, 113, 1237–1240; *Angew. Chem. Int. Ed.* 2001, 40, 1197–1200; c) C. Claver, E. Fernandez, A. Gillon, K. Heslop, D. J. Hyett, A. Martorell, A. G. Orpen, P. G. Pringle, *Chem. Commun.* 2000, 961–962; d) M. T. Reetz, G. Mehler, *Angew. Chem.* 2000, 112, 4047–4049; *Angew. Chem. Int. Ed.* 2000, 39, 3889–3890; e) M. van den Berg, A. J. Minnaard, E. P. Schudde, J. van Esch, A. H. M. de Vries, J. G. de Vries, B. L. Feringa, *J. Am. Chem. Soc.* 2000, 122, 11539–11540.

- [3] a) L. Lefort, J. A. F. Boogers, A. H. M. de Vries, J. G. de Vries, *Org. Lett.* **2004**, 6, 1733–1735; b) J. G. de Vries, L. Lefort, *Chem. Eur. J.* **2006**, 12, 4722–4734; c) C. Jäkel, R. Paciello, *Chem. Rev.* **2006**, 106, 2912–2942.
- [4] a) M. T. Reetz, T. Sell, A. Meiswinkel, G. Mehler, *Angew. Chem.* **2003**, 115, 814–817; *Angew. Chem. Int. Ed.* **2003**, 42, 790–793; b) D. Peña, A. J. Minnaard, J. A. F. Boogers, A. H. M. de Vries, J. G. de Vries, B. L. Feringa, *Org. Biomol. Chem.* **2003**, 1, 1087–1089.
- [5] D. Peña, A. J. Minnaard, A. H. M. de Vries, J. G. de Vries, B. L. Feringa, *Org. Lett.* **2003**, 5, 475–478.
- [6] a) A. J. Minnaard, B. L. Feringa, L. Lefort, J. G. de Vries, *Acc. Chem. Res.* **2007**, 40, 1267–1277, and references therein; b) L. Eberhardt, D. Armspach, J. Harrowfield, D. Matt, *Chem. Soc. Rev.* **2008**, 37, 839–864; c) D. J. Ager, L. Lefort, J. G. de Vries, *ACS Symp. Ser.* **2009**, 1009, 239–250.
- [7] J. A. F. Boogers, U. Felfer, M. Kotthaus, L. Lefort, G. Steinbauer, A. H. M. de Vries, J. G. de Vries, *Org. Process Res. Dev.* **2007**, 11, 585–591.
- [8] M. T. Reetz, A. Meiswinkel, G. Mehler, K. Angermund, M. Graf, W. Thiel, R. Mynott, D. G. Blackmond, *J. Am. Chem. Soc.* **2005**, 127, 10305–10313.
- [9] Y. Fu, X.-X. Guo, S.-F. Zhu, A.-G. Hu, J.-H. Xie, Q.-L. Zhou, *J. Org. Chem.* **2004**, 69, 4648–4655.
- [10] I. D. Gridnev, C. Fan, P. G. Pringle, *Chem. Commun.* **2007**, 1319–1321.
- [11] M. van den Berg, A. J. Minnaard, R. M. Haak, M. Leeman, E. P. Schudde, A. Meetsma, B. L. Feringa, A. H. M. de Vries, C. E. P. Maljaars, C. E. Willans, D. Hyett, J. A. F. Boogers, H. J. W. Henderickx, J. G. de Vries, *Adv. Synth. Catal.* **2003**, 345, 308–323.
- [12] A. Preetz, C. Fischer, C. Kohrt, H.-J. Drexler, W. Baumann, D. Heller, *Organometallics*, DOI: 10.1021/om200486t.
- [13] a) D. A. Evans, F. E. Michael, J. S. Tedrow, K. R. Campos, *J. Am. Chem. Soc.* **2003**, 125, 3534–3543; b) H.-J. Drexler, W. Baumann, T. Schmidt, S. Zhang, A. Sun, A. Spannenberg, C. Fischer, H. Bauschmann, D. Heller, *Angew. Chem.* **2005**, 117, 1208–1212; *Angew. Chem. Int. Ed.* **2005**, 44, 1184–1188; c) for a recent discussion of the Major/Minor concept, see: T. Schmidt, Z. Dai, H.-J. Drexler, M. Hapke, A. Preetz, D. Heller, *Chem. Asian J.* **2008**, 3, 1170–1180.
- [14] a) A. S. C. Chan, J. J. Pluth, J. Halpern, *J. Am. Chem. Soc.* **1980**, 102, 5952–5954; b) J. Halpern, *Science* **1982**, 217, 401–407; c) J. Halpern in *Chiral Catalysis*, Vol. 5 (Ed.: J. D. Morrison), Academic Press, Orlando, **1985**, pp. 41–69; d) C. R. Landis, J. Halpern, *J. Am. Chem. Soc.* **1987**, 109, 1746–1754; e) B. McCulloch, J. Halpern, M. R. Thompson, C. R. Landis, *Organometallics* **1990**, 9, 1392–1395; f) T. Schmidt, W. Baumann, H.-J. Drexler, A. Arrieta, D. Heller, H. Buschmann, *Organometallics* **2005**, 24, 3842–3848; g) T. Schmidt, Z. Dai, H.-J. Drexler, W. Baumann, C. Jäger, D. Pfeifer, D. Heller, *Chem. Eur. J.* **2008**, 14, 4469–4471.
- [15] M. van den Berg, Ph.D. Thesis, University of Groningen (The Netherlands), **2006**; <http://dissertations.ub.rug.nl/faculties/science/2006m.van.den.berg/>.
- [16] P. Jankowski, C. L. McMullin, I. D. Gridnev, A. G. Orpen, P. P. Pringle, *Tetrahedron: Asymmetry* **2010**, 21, 1206–1209.
- [17] N. B. Johnson, I. C. Lennon, P. H. Moran, J. A. Ramsden, *Acc. Chem. Res.* **2007**, 40, 1291–1299.
- [18] R. R. Schrock, J. A. Osborn, *Inorg. Chem.* **1971**, 10, 2397–2407.
- [19] The X-ray structure of this species has been already reported in Ref. [11], so it is not included in this paper. However, the X-ray analysis served to unambiguously assign its structure as the solution NMR spectra are fairly complicated.
- [20] Even with BisP* ligands (BisP* = 1,2-bis(alkylmethylphosphino)ethanes, alkyl = *tert*-butyl-1-adamantyl, 1-methylcyclohexyl, 1,1-diethylpropyl, cyclopentyl, cyclohexyl, isopropyl), the relative amount of rhodium complexes that contain four-coordinated phosphorus donors prevails if the catalyst precursors are prepared from [Rh(cod)₂][BF₄] relative to [Rh(nbd)₂][BF₄]: I. D. Gridnev, Y. Yamanoi, N. Higashi, H. Tsuruta, M. Yasutake, T. Imamoto, *Adv. Synth. Catal.* **2001**, 343, 118–136.
- [21] Dichloroethane has been used in place of dichloromethane because the latter is a poorly suited solvent for running kinetic investigations at 1 bar total pressure due to its high vapour pressure. In dichloroethane, the same intermediates as found in dichloromethane have been detected by NMR spectroscopy.
- [22] D. Heller, A. H. M. de Vries, J. G. de Vries in *Handbook of Homogeneous Hydrogenation*, Vol. 3 (Eds.: J. G. de Vries, C. J. Elsevier), Wiley-VCH, Weinheim, **2007**, pp. 1483–1516.
- [23] a) J. M. Ernsting, S. Gaemers, C. J. Elsevier, *Magn. Reson. Chem.* **2004**, 42, 721–736; b) W. von Philipsborn, *Chem. Soc. Rev.* **1999**, 28, 95–105.
- [24] Although the complexes have a different counterion, the comparison is still appropriate as it has been shown that non-coordinating anions affect very weakly the ¹⁰³Rh chemical shift of the corresponding complexes: A. Fabrello, C. Dinoi, L. Perrin, P. Kalck, L. Maron, M. Urrutigoity, O. Dechy-Cabaret, *Magn. Reson. Chem.* **2010**, 48, 848–856.
- [25] D. Heller, H.-J. Drexler, A. Spannenberg, B. Heller, J. You, W. Baumann, *Angew. Chem.* **2002**, 114, 814–817; *Angew. Chem. Int. Ed.* **2002**, 41, 777–780.
- [26] The possibility for phosphoramidite ligands to act as multidentate ligands through dangling aromatic substituents (η^2 or η^6) and phosphorus has been previously described, see T. Osswald, H. Rüegger, A. Mezzetti, *Chem. Eur. J.* **2010**, 16, 1388–1397, and references therein.
- [27] Similar dimeric species have been reported with the following phosphine ligands: DPPE: a) J. Halpern, D. P. Riley, A. S. C. Chan, J. J. Pluth, *J. Am. Chem. Soc.* **1977**, 99, 8055–8057; b) D. P. Fairlie, B. Bosnich, *Organometallics* **1988**, 7, 936–945; c) D. P. Fairlie, B. Bosnich, *Organometallics* **1988**, 7, 946–954; DIPAMP: d) A. Preetz, W. Baumann, C. Fischer, H.-J. Drexler, T. Schmidt, R. Thede, D. Heller, *Organometallics* **2009**, 28, 3673–3677; CYCPOS: e) D. P. Riley, *J. Organomet. Chem.* **1982**, 234, 85–97; DIPH: f) D. G. Allen, S. B. Wild, D. L. Wood, *Organometallics* **1986**, 5, 1009–1015; CHIRAPHOS: g) S. H. Bergens, P. Noheda, J. Whelan, B. Bosnich, *J. Am. Chem. Soc.* **1992**, 114, 2121–2128; h) R. W. Barnhart, X. Wang, P. Noheda, S. H. Bergens, J. Whelan, B. Bosnich, *Tetrahedron* **1994**, 50, 4335–4346; SKEWPHOS: i) K. Mikami, Y. Yusa, M. Hatano, K. Wakabayashi, K. Aikawa, *Chem. Commun.* **2004**, 98–99; BIPHEP: j) K. Mikami, S. Kataoka, Y. Yusa, K. Aikawa, *Org. Lett.* **2004**, 6, 3699–3701; P(*p*Tolyl)₃: k) P. Marazzan, M. B. Ezhova, B. O. Patrick, B. R. James, *C. R. Chim.* **2002**, 5, 373–378; Monophosphonite: reference [10].
- [28] In the case of binaphthol-based monophosphonites (see Ref. [10]) in dichloroethane, the dimer is in equilibrium with the solvato species, the relative concentrations being dependent on the total rhodium concentration in solution.
- [29] A different behaviour is expected in a coordinating solvent (see Ref. [27k]): when hydrogenation of **8a** is carried out in MeOH under otherwise identical conditions the dimer is not observed. The ³¹P NMR spectrum shows a broad absorption centred around δ = 154 ppm, which might point to rapidly interconverting solvato or hydride species.
- [30] R. R. Schrock, J. A. Osborn, *J. Am. Chem. Soc.* **1976**, 98, 2134–2143: Rhodium complexes [Rh(L)₂(nbd)]BF₄ that contain monophosphines such as PPh₃, PMePh₂ and PMe₂Ph upon hydrogenation in a coordinating solvent at room temperature give rise to stable dihydrides that could be isolated and characterised. According to Halpern (Ref. [27a]) the stability of such dihydrides might be ascribed to the fact that, because of the presence of monophosphines, in the dihydride neither hydrogen ligand needs to be *trans* to a phosphine (assuming a *cis* disposition of the two hydrogen atoms).
- [31] a) J. M. Brown, P. A. Chaloner, P. N. Nicholson, *J. Chem. Soc. Chem. Commun.* **1978**, 646–647; b) J. M. Brown, P. A. Chaloner, A. G. Kent, B. A. Murrer, P. N. Nicholson, D. Parker, P. J. Sidebottom, *J. Organomet. Chem.* **1981**, 216, 263–276; no stable hydrides were detected when using ligand (*R*)-(o-methoxyphenyl)phenylmethylphosphine, which probably acts as a chelating ligand through the *ortho*-methoxy group.

- [32] a) J. M. Brown, P. A. Chaloner, *Tetrahedron Lett.* **1978**, *19*, 1877–1880; b) A. S. C. Chan, J. J. Pluth, J. Halpern, *Inorg. Chim. Acta* **1979**, *37*, L477–L479; c) A. S. C. Chan, J. Halpern, *J. Am. Chem. Soc.* **1980**, *102*, 838–840; d) J. M. Brown, P. A. Chaloner, *J. Am. Chem. Soc.* **1980**, *102*, 3040–3048; e) J. M. Brown, P. A. Chaloner, *J. Chem. Soc. Chem. Commun.* **1980**, 344–346; f) I. Ojima, T. Kogure, N. Yoda, *J. Org. Chem.* **1980**, *45*, 4728–4739; g) J. M. Brown, D. Parker, *J. Org. Chem.* **1982**, *47*, 2722–2730.
- [33] In the case of the analogous adducts of rhodium–monophosphonite complex, no indication of the formation of a chelated substrate complex was gained from NMR spectra, and only a doublet was observed in the ^{31}P NMR spectrum. By the use of labelled $\alpha\text{-}^{13}\text{C}$ methyl α -benzoyloxyethenephosphonate, a strongly chelating substrate to $[\text{Rh}(\text{diphosphine})(\text{Solv})_2]^+$ fragments, it was proven instead that, if the ligand is *t*BuP(binaphthoxo), this substrate is only weakly monocoordinated through the phosphoryl oxygen (see Ref. [10]).
- [34] a) H. Bircher, B. R. Bender, W. von Philipsborn, *Magn. Reson. Chem.* **1993**, *31*, 293–298; b) J. M. Brown, P. A. Chaloner, G. A. Morris, *J. Chem. Soc. Chem. Commun.* **1983**, 664–666; c) J. M. Brown, P. A. Chaloner, G. A. Morris, *J. Chem. Soc. Perkin Trans. 2* **1987**, 1583–1588; d) J. A. Ramsden, T. D. W. Claridge, J. M. Brown, *J. Chem. Soc. Chem. Commun.* **1995**, 2469–2471; e) R. Kadyrov, T. Freier, D. Heller, M. Michalik, R. Selke, *J. Chem. Soc. Chem. Commun.* **1995**, 1745–1746; f) D. Heller, R. Kadyrov, M. Michalik, T. Freier, U. Schmidt, H. W. Krause, *Tetrahedron: Asymmetry* **1996**, *7*, 3025–3035.
- [35] B. R. Bender, M. Koller, D. Nanz, W. von Philipsborn, *J. Am. Chem. Soc.* **1993**, *115*, 5889–5890.
- [36] I. D. Gridnev, N. Higashi, K. Asakura, T. Imamoto, *J. Am. Chem. Soc.* **2000**, *122*, 7183–7194.
- [37] J. M. Buriak, J. A. Osborn, *J. Chem. Soc. Chem. Commun.* **1995**, 689–690.
- [38] a) C. R. Landis, P. Hilfenhaus, S. Feldgus, *J. Am. Chem. Soc.* **1999**, *121*, 8741–8754; b) A. L. Sargent, M. B. Hall, M. F. Guest, *J. Am. Chem. Soc.* **1992**, *114*, 517–522.
- [39] G. Giordano, R. H. Crabtree, *Inorg. Synth.* **1990**, *28*, 88–90.
- [40] R. R. Schrock, J. A. Osborn, *J. Am. Chem. Soc.* **1971**, *93*, 3089–3091.

Received: June 11, 2011

Published online: September 28, 2011